

Deep Graph-neighbor Coherence Preserving Network for Unsupervised Cross-modal Hashing

Jun Yu^{1*}, Hao Zhou¹, Yibing Zhan¹, Dacheng Tao²

¹ HangZhou Dianzi University

² The University of Sydney

yujun@hdu.edu.cn, zhouhao@hdu.edu.cn, zybji@hdu.edu.cn, dacheng.tao@sydney.edu.au

Abstract

Unsupervised cross-modal hashing (UCMH) has become a hot topic recently. Current UCMH focuses on exploring data similarities. However, current UCMH methods calculate the similarity between two data, mainly relying on the two data’s cross-modal features. These methods suffer from inaccurate similarity problems that result in a suboptimal retrieval Hamming space, because the cross-modal features between the data are not sufficient to describe the complex data relationships, such as situations where two data have different feature representations but share the inherent concepts. In this paper, we devise a deep graph-neighbor coherence preserving network (DGCPN). Specifically, DGCPN stems from graph models and explores graph-neighbor coherence by consolidating the information between data and their neighbors. DGCPN regulates comprehensive similarity preserving losses by exploiting three types of data similarities (i.e., the graph-neighbor coherence, the coexistent similarity, and the intra- and inter-modality consistency) and designs a half-real and half-binary optimization strategy to reduce the quantization errors during hashing. Essentially, DGCPN addresses the inaccurate similarity problem by exploring and exploiting the data’s intrinsic relationships in a graph. We conduct extensive experiments on three public UCMH datasets. The experimental results demonstrate the superiority of DGCPN, e.g., by improving the mean average precision from 0.722 to 0.751 on MIRFlickr-25K using 64-bit hashing codes to retrieve texts from images. We will release the source code package and the trained model on <https://github.com/Atmegal/DGCPN>.

Introduction

Cross-modal retrieval (CMR) aims to retrieve relevant data when given queries that have different modalities of the retrieval data (Wang et al. 2016). Due to the explosion of multimedia data on the Internet (Yu, Rui, and Chen 2013; Yang et al. 2020c), cross-modal retrieval has become an essential technique in information retrieval (Yang et al. 2020c) and multi-modal data mining (Qiao et al. 2019b,a; Yang et al. 2020a,c; Li et al. 2020). Generally, CMR methods map heterogeneous data into a common space. In this common space, similarities between data can be directly measured. However, most CMR methods use real-valued com-



Figure 1: Cross-modal examples of three images and their coexistent tags. Rose and wedding have high similarities because the rose is a fundamental component of a wedding. However, this intricate relationship cannot be derived by using visual appearances and linguistic tags of the given “rose” and “wedding”. Nevertheless, such a connection can be inferred by their neighbor coherence that both “rose” and “wedding” have high similarities of the “bride, rose”.

mon spaces, and they suffer from high computation burden for a large volume of multimedia data (Feng, Wang, and Li 2014; Wang et al. 2017; Xie et al. 2020). By contrast, cross-modal hashing (CMH) methods use compact Hamming space. Due to lower data storage and higher retrieval efficiency, CMH methods have become a hot topic recently.

CMH methods can be roughly classified into two categories: supervised methods (Jiang and Li 2017) and unsupervised methods (Su, Zhong, and Zhang 2019). Supervised methods require semantic labels, whereas unsupervised methods only need to know whether heterogeneous data are coexistent (Wang et al. 2016). In most real-world situations, semantic labels are unavailable, and manual annotations are time-consuming and expensive; and consequently, unsupervised CMH (UCMH) methods are more flexible and feasible.

Current UCMH methods focused on generating data similarities that reflect the data’s semantic relationships. They used data similarities as optimization targets to preserve data similarities during hashing (Su, Zhong, and Zhang 2019; Yang et al. 2020b; Liu et al. 2020). Although current UCMH methods achieved promising improvements, they still suffer from inaccurate similarity problems, limiting retrieval performance. Most methods calculate similarities between data, using features only between the corresponding two

*Jun Yu is the corresponding author

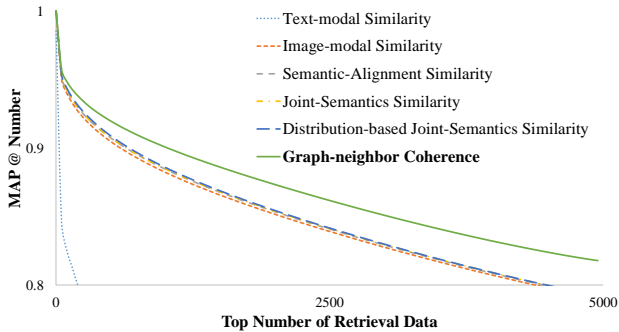


Figure 2: Comparison of six types of data similarities using 5000 data on MIRFlickr-25K (Huiskes and Lew 2008). MAP@Number is the mean average precision (MAP) based on the top number of retrieval data. Following (Hu et al. 2020), we use a pre-trained VGG-19 (Simonyan and Zisserman 2014) to extract image features and use the bag-of-words (BoW) model to extract text features. Text-modal and image-modal similarities are cosine similarities using the text and image features. Semantic-alignment similarity (Yang et al. 2020b) fuses text and image modal similarities. Both joint-semantics similarity (Su, Zhong, and Zhang 2019) and distribution-based joint-semantics similarity (Yang et al. 2020b) additionally exploit data distributions. Graph-neighbor coherence is the similarity proposed in this paper. We can conclude that graph-neighbor coherence has the best consistency with the real similarities of labels.

data (Yang et al. 2020b). However, features between data are insufficient to describe intricate data relationships; for example, rose and wedding have higher similarities because the rose is the basic component of the wedding. Nevertheless, this relationship cannot be derived from visual appearances and linguistic tags of the given “rose” and “wedding” in Fig. 1. Intuitively, such high similarity can be inferred from their coherence of neighbors, i.e., both “rose” and “wedding” have high similarities of the “bride and rose.”

Even though some methods attempt to consider data distribution (Su, Zhong, and Zhang 2019; Liu et al. 2020), the similarities of these methods are calculated, mainly relying on the features between the data; their similarities still have huge gaps compared with the real situations derived from labels. Fig. 2 compares the mean average precision (MAP) of six types of data similarities using 5000 data of MIRFlickr-25K (Huiskes and Lew 2008). Text-modal and image-modal similarities are obtained using single modal features. Semantic-alignment similarity (Yang et al. 2020b) fuses text and image modal similarities. Both joint-semantics similarity (Su, Zhong, and Zhang 2019) and distribution-based joint-semantics similarity (Liu et al. 2020) consider data distributions. Graph-neighbor coherence is the similarity proposed in this paper. We observe that previous data similarities only slightly outperform the image-model similarities.

In light of the above analysis, we develop a deep graph-neighbor coherence preserving network (DGCPN) for

UCMH that has the following main contributions:

- We propose graph-neighbor coherence (GC) that explores the relationships between data and their neighbors. Specifically, we model the retrieval data as a graph in which each node consists of a group of coexistent data; naturally, the similarities between data are equal to the similarities between the corresponding nodes. The GC is calculated based on a designed conditional probability model that sums all probabilities of whether both two calculating nodes have high similarities of one of their common neighbors. In this manner, GC considers not only the number of common neighbors but also the similarity degree of the neighbors between the two nodes. Here, we suppose that each node is connected to k -nearest neighbors (k -NN) and obtain the two nodes’ probabilities with high similarities using the two nodes’ cross-modal features. GC further adds the distance between nodes for robust performance. As shown in Fig. 2, GC effectively reflects the data retrieval relationships and thus addresses the inaccurate similarity problem.
- DGCPN designs comprehensive similarity preserving losses to regulate three types of similarities: 1) graph-neighbor coherence between data in a subset, 2) coexistent similarity between coexistent data, and 3) intra- and inter-modality consistency between similarities obtained from different modalities. The comprehensive similarity preservation guarantees the robust learning process, and the intrinsic relationships of data (i.e., the coexistent similarity and the intra- and inter-modality consistency) alleviate the side effects of graph-neighbor coherence’s possible inaccurate similarities.
- Moreover, DGCPN develops a half-real and half-binary optimization strategy to reduce the value gaps and the similarity gaps between the real-valued space and Hamming space by calculating the losses between one real value and one binary code. The optimization strategy effectively reduces quantization errors during hashing.

We conducted extensive experiments on three public datasets. The improved performance compared with the state-of-the-art demonstrates the competitiveness of DGCPN. The rest of the paper is organized as follows: we first review related works. Then, we explain the details of DGCPN and present the experimental results. The last section concludes this paper.

Related UCMH Work

Previous UCMH methods focused on obtaining binary codes of data and learned the hashing functions by mapping data features into the corresponding binary codes (Liong, Lu, and Tan 2018). For example, IMH (Song et al. 2013), CMFH (Ding, Guo, and Zhou 2014), and MSFH (Fang, Zhang, and Ren 2019) learned hashing codes by preserving intra- and inter-graph consistency, using collective matrix factorization, and using multigraph regularized smooth matrix factorization, respectively. However, the above methods were space-consuming because obtaining robust binary codes requires considering all training data simultaneously. Besides,

most previous methods used human-crafted features and shallow models that limited the retrieval performance.

Later, UCMH methods exploited deep neural networks (DNNs) (Wang et al. 2020; Zhang and Tao 2020). For example, Hu, Nie, and Li designed a deep autoencoder with an adjusted Tanh function. Li et al. and Zhang and Peng proposed coupled cycle generative adversarial networks (GANs) and multi-pathway GANs, respectively. Some UCMH methods learned real values with approximate binary representations and obtained the binary codes from the real values using a Sign function (Kumar and Udupa 2011). Most deep methods adopted the above strategy to implement batch-wise training to save time and space (Wang et al. 2020; Hu et al. 2020).

In UCMH, data similarities serve as critical considerations (Liang et al. 2016; Li et al. 2017). Earlier UCMH methods calculated data similarities by using discrete models (Song et al. 2013; Ding, Guo, and Zhou 2014). For instance, data pairs with smaller and larger feature distances were set to 1 and -1, respectively (Kumar and Udupa 2011). However, discrete models ignore the data pairs with intermediate distances. Later, continuous similarities between data were designed by using feature distances (Xie, Zhu, and Chen 2016; Fang, Zhang, and Ren 2019). Nevertheless, the data similarities have been generally used as weights in the optimization functions and did not make full use of data similarities (Wu et al. 2018; Wang et al. 2020; Hu et al. 2020). Most current methods learned retrieval Hamming space by preserving calculated data similarities. Su, Zhong, and Zhang, Yang et al., and Liu et al. adopted semantic-alignment similarities fusing cross-modal information. Moreover, Su, Zhong, and Zhang and Liu et al. considered structural information. However, recent UCMH methods still suffer from inaccurate similarity problems and obtain suboptimal retrieval Hamming space.

DGCPN

This section presents the proposed DGCPN. Specifically, we first introduce the framework and preliminary definitions. We then explain the details of the graph-neighbor coherence, the comprehensive similarity preserving losses, and the half-real and half-binary optimization strategy sequentially.

The Framework and Preliminary Definitions

Fig. 3 presents the framework of DGCPN. Without loss of generality, we use texts and images as the cross-modal examples. The blue background illuminates the network details. Specifically, DGCPN consists of two sequential subnetworks: feature-extracting subnetworks to extract the image and text features and similarity-preserving subnetworks to map the image and text features into binary codes. We note that the feature-extracting subnetworks can marry other backbones, such as AlexNet (Krizhevsky, Sutskever, and Hinton 2012) and the Latent Dirichlet allocation (LDA) model (Blei, Ng, and Jordan 2003). The green background shows the training details. Specifically, the GC between data is first obtained by analyzing the whole training data. Then, DGCPN is trained in a batch-wise manner based on the designed comprehensive similarity preserving losses. Moreover, we exploit a half-real and half-binary optimization strategy to further improve retrieval performance.

Suppose (v_i, t_i) indicate the i -th coexistent image and text. $i \in [M]$. We define $[M]=\{1, 2, \dots, M\}$. M is the total number of coexistent pairs. The features, relaxed real values, and binary codes of the i -th image and text are defined as $\vec{f}_{*i} \in \mathbb{R}^{d_* \times 1}$, $\vec{h}_{*i} \in \mathbb{R}^{d_b \times 1}$, and $\vec{b}_{*i} \in \mathbb{R}^{d_b \times 1}$, respectively. $* \in \{I, T\}$. d_I , d_T , and d_b are the dimension of image features, text features, and hashing coding, respectively. $\vec{b}_{*i} = \text{sign}(\vec{h}_{*i})$. The $\text{sign}(\cdot)$ is the Sign function. DGCPN adopts batch-wise training. Suppose $\mathbf{F}_* = \{\vec{f}_{*i}, i \in [N]\} \in \mathbb{R}^{d_* \times N}$, $\mathbf{H}_* = \{\vec{h}_{*i}, i \in [N]\} \in \mathbb{R}^{d_b \times N}$, and $\mathbf{B}_* = \{\vec{b}_{*i}, i \in [N]\} \in \mathbb{R}^{d_b \times N}$ indicate a set of features, relaxed real values, and binary codes with the batchsize of N , respectively. Besides,

$$\mathbf{H}_I = \text{ImgNet}(\mathbf{F}_I, \theta_I) \text{ and } \mathbf{H}_T = \text{TxtNet}(\mathbf{F}_T, \theta_T), \quad (1)$$

where θ_I and θ_T are training parameters.

We use cosine similarity to measure the similarity (or distance) between vectors. The cosine similarity is defined as:

$$c(\vec{x}_i, \vec{x}_j) = \frac{\vec{x}_i^T \vec{x}_j}{\|\vec{x}_i\|_2 \|\vec{x}_j\|_2}, \quad (2)$$

where \vec{x}_i^T is the transpose of \vec{x}_i . $\|\cdot\|_2$ is the L2-norm of vectors. We select cosine similarity because cosine similarity is commonly adopted in deep UCMH methods (Yang et al. 2020b; Liu et al. 2020). The cosine similarities between two sets of vectors are defined as follows:

$$\mathbf{C}(\mathbf{X}, \mathbf{X}) = \begin{bmatrix} c(\vec{x}_1, \vec{x}_1) & c(\vec{x}_1, \vec{x}_2) & \cdots & c(\vec{x}_1, \vec{x}_N) \\ c(\vec{x}_2, \vec{x}_1) & c(\vec{x}_2, \vec{x}_2) & \cdots & c(\vec{x}_2, \vec{x}_N) \\ \vdots & \vdots & \ddots & \vdots \\ c(\vec{x}_N, \vec{x}_1) & c(\vec{x}_N, \vec{x}_2) & \cdots & c(\vec{x}_N, \vec{x}_N) \end{bmatrix}, \quad (3)$$

where $\mathbf{X} = \{\vec{x}_i, i \in [N]\}$.

Graph-neighbor Coherence

As aforementioned, previous methods generally calculated similarities between data, mainly relying on the two data's cross-modal features; and current data similarities still have huge gaps compared with the real similarities obtained from labels. DGCPN proposes graph-neighbor coherence (GC) that improves the accuracy of previous data similarities by combining cross-modal features between two data and relationships between the two data and their neighbors. This subsection introduces the details of GC.

Specifically, we model all of the training data as a graph $\mathcal{G} = \{\mathcal{O}, \mathcal{E}\}$. $\mathcal{O} = \{o_i, i \in [M]\}$. $o_i = (v_i, t_i)$. Suppose l_i indicates the label of v_i , t_i , and o_i . Therefore, the problem of calculating similarities between the data is transformed into calculating similarities between the nodes. We model GC between the nodes as a conditional probability problem:

$$P(l_i = l_j) = P(l_i = l_j | \mathcal{O}). \quad (4)$$

However, the calculation of GC based on Eq. (4) is complicated because there are M joint variables that constitute numerous conditional combinations. For computational efficiency, we impose the limitation in calculating GC between

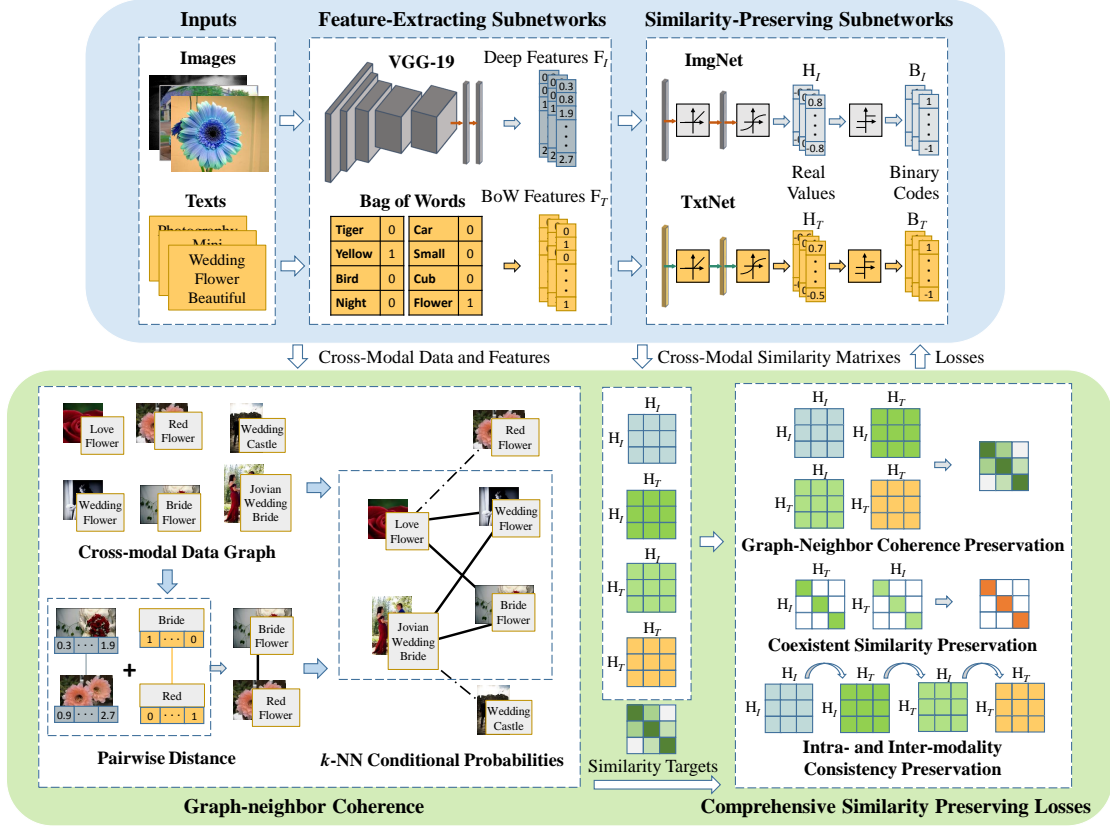


Figure 3: The framework of DGCPN. The blue background illuminates the network details. Specifically, DGCPN first extracts image and text features by using feature-extracting subnetworks. Afterward, DGCPN maps the image and text features into relaxed real values and binary codes using similarity-preserving subnetworks. The green background shows additional training details. During training, the graph-neighbor coherence of training data are calculated by analyzing cross-modal data features. Then, DGCPN is trained by calculating the comprehensive similarity preserving losses based on a batch size of data.

two nodes that only one other node is used as a condition. According to the total probability rule, Eq. (4) is revised as:

$$P(l_i = l_j) = \sum_{q=1}^M P(l_i^F = l_q^F | o_i, o_q) P(l_j^F = l_q^F | o_j, o_q), \quad (5)$$

where l_*^F is the virtual label of o_* . We use virtual labels to discuss the similarities between nodes. $P(l_i^F = l_q^F | o_i, o_q)$ indicates the probability that o_i and o_q have the same virtual labels or have higher similarities. We suppose each node is related to its k -nearest neighbors and following Zhai, Peng, and Xiao; Zhan et al. define $P(l_i^F = l_q^F | o_i, o_q)$ as:

$$P(l_i^F = l_q^F | o_i, o_q) = \begin{cases} \frac{d(o_i, o_q)}{\sum_{p \in \mathbf{Ne}(o_i, k)} d(o_i, o_p)} & o_q \in \mathbf{Ne}(o_i, k) \\ 0 & \text{else} \end{cases}, \quad (6)$$

where $d(o_i, o_q)$ is the pairwise distance between o_i and o_q :

$$d(o_i, o_q) = (1 - \alpha)c(\vec{f}_{I_i}, \vec{f}_{I_q}) + \alpha c(\vec{f}_{T_i}, \vec{f}_{T_q}), \quad (7)$$

and $\mathbf{Ne}(o_i, k)$ indicates the set of k -nearest neighbors of o_i using Eq. (7). Note that $c(\vec{f}_{I_i}, \vec{f}_{I_q})$, $c(\vec{f}_{T_i}, \vec{f}_{T_q})$, and

$d(o_i, o_q)$ are in the 0-1 range because of the adopted deep features and BoW features. The graph-neighbor coherence between o_i and o_j is calculated as:

$$s(o_i, o_j) = (1 - \gamma)d(o_i, o_j) + \gamma\beta P(l_i = l_j), \quad (8)$$

where β is used to adjust the range of $P(l_i = l_j)$. γ is a trade off parameter. We add $d(o_i, o_j)$ for robust performance. We note that the cosine similarity values range between -1 to 1. Therefore, following Liu et al., we use $2s(o_i, o_k) - 1$ as the final graph-neighbor coherence during training.

Comprehensive Similarity Preserving Losses

Current methods have mainly focused on preserving similarities and rarely proposed solutions to solve the inaccurate similarity problem. By contrast, DGCPN proposes comprehensive similarity preserving losses by maintaining data similarities from three complementary aspects: graph-coherence preservation, coexistent similarity preservation, and intra- and inter-modality consistency preservation. The three types of complementary similarity preservation guarantee the robust similarity learning process. The exploitation of the intrinsic relationships between the data (i.e., the

coexistent similarity and the intra- and inter-modality consistency) alleviates the side effect of inaccurate similarities.

Suppose that there exists a batch size of training data with relaxed real values: \mathbf{H}_I and \mathbf{H}_T . Then, four types of similarity matrixes are generated, namely, two homogeneous data similarity matrixes: $\mathcal{C}(\mathbf{H}_I, \mathbf{H}_I)$, $\mathcal{C}(\mathbf{H}_T, \mathbf{H}_T)$ and two heterogeneous data similarities matrixes: $\mathcal{C}(\mathbf{H}_I, \mathbf{H}_T)$, $\mathcal{C}(\mathbf{H}_T, \mathbf{H}_I)$.

The graph-neighbor coherence preserving losses $L_g(\mathbf{H}_I, \mathbf{H}_T)$, the coexistent similarity preserving losses $L_c(\mathbf{H}_I, \mathbf{H}_T)$, and the intra- and inter-modality consistency preserving losses $L_i(\mathbf{H}_I, \mathbf{H}_T)$ are respectively defined as:

$$L_g(\mathbf{H}_I, \mathbf{H}_T) = \sum_{p,q} \|\mathcal{C}(\mathbf{H}_p, \mathbf{H}_q) - S_{gc}(\mathbf{H}_I, \mathbf{H}_T)\|_F, \quad (9)$$

$$L_c(\mathbf{H}_I, \mathbf{H}_T) = \|\text{Tr}(\mathcal{C}(\mathbf{H}_I, \mathbf{H}_T) - 1.5\mathbf{I})\|_2, \quad (10)$$

$$L_i(\mathbf{H}_I, \mathbf{H}_T) = \sum_{p,q,p_1,q_1} \|\mathcal{C}(\mathbf{H}_p, \mathbf{H}_q) - \mathcal{C}(\mathbf{H}_{p_1}, \mathbf{H}_{q_1})\|_F, \quad (11)$$

where $p, q, p_1, q_1 \in \{I, T\}$. $S_{gc}(\mathbf{H}_I, \mathbf{H}_T)$ is the corresponding GC of $\mathbf{H}_I, \mathbf{H}_T$. $\|\cdot\|_F$ is the Frobenius norm. \mathbf{I} is an identity matrix with the same size of $\mathcal{C}(\mathbf{H}_I, \mathbf{H}_T)$. Following Liu et al., we use 1.5 as the optimization goal of the coexistent similarity preserving that slightly improves performance. $\text{Tr}(\cdot)$ is the matrix trace. For simplicity, we set all similarity matrixes to have the same significance.

Graph-neighbor coherence reflects the similarities of whether two data share the same labels and is used as the supervised information in $L_g(\mathbf{H}_I, \mathbf{H}_T)$. However, the GC may still obtain errors. Intuitively, the coexistent similarities between coexistent data should be high; and the intra- and inter-modality consistency represents that data's similarities should equal the corresponding nodes' similarities, regardless of the data's modalities. Both the coexistent similarities and intra- and inter-modality consistency are intrinsic data relationships. Therefore, the exploitation of the coexistent similarity and intra- and inter-modality consistency alleviates the side effect of GC's possible errors.

The final similarity preserving losses are calculated as:

$$L(\mathbf{H}_I, \mathbf{H}_T) = L_c(\mathbf{H}_I, \mathbf{H}_T) + \lambda_1 L_g(\mathbf{H}_I, \mathbf{H}_T) + \lambda_2 L_i(\mathbf{H}_I, \mathbf{H}_T), \quad (12)$$

where λ_1 and λ_2 are the parameters used to adjust the relative significance of the three similarity preserving losses.

Half-real and Half-binary Optimization Strategy

Previous methods only reduce the value gaps between relaxed real values and binary codes. They still ignore the similarity gaps between the real-valued space and Hamming space. DGCPN proposes a half-real and half-binary optimization strategy to reduce both value gaps and similarity gaps. Intuitively, DGCPN reduces both gaps by additionally preserving similarities in the Hamming space. However, learning with pure binary codes is difficult. Therefore, we relax this condition by calculating similarities between one real value and one binary code. Specifically, we use $L(\mathbf{H}_I, \mathbf{H}_T)$ to train the whole networks. Then, we use

Algorithm 1 Graph-neighbor Coherence Preserving

Input:

M Training Images and Texts; Validation Images and Texts; Batch size N ; hash code length d_b ; Max training epoch E ; trade-off parameters $\alpha, \gamma, \lambda_1$, and λ_2 ; k -nearest number and scale parameter β ;

Output:

Hashing Function $\text{ImgNet}(\cdot, \theta_I)$ and $\text{TtxtNet}(\cdot, \theta_T)$;

- 1: Initial θ_I and θ_T ;
 - 2: Extract image and text features of Training set and obtain graph-neighbor coherence of all training data;
 - 3: **for** each $i \in [1, E]$ **do**
 - 4: **for** each $j \in [1, M/N]$ **do**
 - 5: obtain training data with batch size of N and the corresponding $S_{gc}(\mathbf{H}_I, \mathbf{H}_T)$;
 - 6: update θ_I and θ_T using $L(\mathbf{H}_I, \mathbf{H}_T)$;
 - 7: update θ_I using $L(\mathbf{H}_I, \mathbf{B}_T)$;
 - 8: update θ_T using $L(\mathbf{B}_I, \mathbf{H}_T)$;
 - 9: **end for**
 - 10: calculate MAP of Validation set; if convergence, stop;
 - 11: **end for**
 - 12: **return** $\text{ImgNet}(\cdot, \theta_I)$ and $\text{TtxtNet}(\cdot, \theta_T)$;
-

$L(\mathbf{H}_I, \mathbf{B}_T)$ and $L(\mathbf{B}_I, \mathbf{H}_T)$ to train the networks of images and texts, respectively. The details of the optimization are presented in the Algorithm 1.

Experiments

Datasets and Evaluation Metrics

Three public datasets are adopted in our experiments: Wikipedia (Rasiwasia et al. 2010), MIRFlickr-25K (Huiskes and Lew 2008), and NUS-WIDE (Chua et al. 2009).

Wikipedia dataset consists of 2,866 image-text pairs from 10 categories. We split Wikipedia dataset into the retrieval/test query/validation query set with 2173/462/231 image-text pairs. The whole retrieval set is used for training.

MIRFlickr-25K dataset contains 20,015 image-tag pairs with multi labels from 24 classes. We split MIRFlickr-25K dataset into the retrieval/test query/validation query set with 16,015/2000/2000 image-tag pairs. 5000 image-tag pairs of the retrieval set are used for training.

NUS-WIDE dataset provides 186,577 image-tag pairs with the top-10 concepts. We split NUS-WIDE into retrieval/test query/validation query set with 182,577/2000/2000 image-tag pairs. 5000 image-tag pairs of the retrieval set are used for training. Besides, we select 10,000 image-text pairs from the whole retrieval set as the validation retrieval set for computational efficiency.

Following Hu et al., for all datasets, the images are represented by 4096-dimensional deep features extracted from VGG-19 pretrained on ImageNet (Deng et al. 2009). The text representations of Wikipedia, MIRFlickr-25K, and NUS-WIDE are 10-dimensional LDA, 1386-dimensional BoW, and 1000-dimensional BoW features, respectively.

Two cross-modal retrieval tasks are used for testing: text retrieval from an image query (I2T) and image retrieval from

Task	Method	Wikipedia			MIRFlickr-25K			NUS-WIDE		
		16-bit	32-bit	64-bit	16-bit	32-bit	64-bit	16-bit	32-bit	64-bit
I2T	CVH (Kumar and Udupa 2011)	0.146	0.149	0.155	0.580	0.579	0.579	0.379	0.378	0.377
	FSH (Liu et al. 2017)	0.242	0.283	0.305	0.590	0.597	0.597	0.400	0.414	0.424
	CMFH (Ding, Guo, and Zhou 2014)	0.163	0.176	0.163	0.588	0.592	0.594	0.483	0.488	0.486
	LSSH (Zhou, Ding, and Guo 2014)	0.364	0.387	0.397	0.630	0.634	0.631	0.475	0.484	0.474
	UGACH (Zhang, Peng, and Yuan 2018)	0.319	0.358	0.377	0.686	0.695	0.702	0.568	0.583	0.589
	DJSRH (Su, Zhong, and Zhang 2019)	0.384	0.398	0.406	0.666	0.678	0.699	0.513	0.535	0.566
	UKD-SS (Hu et al. 2020)	0.332	0.344	0.337	0.700	0.706	0.709	0.584	0.578	0.586
	DSAH (Yang et al. 2020b)	0.395	0.409	0.413	0.701	0.712	0.722	0.602	0.612	0.632
JDSH (Liu et al. 2020)	0.351	0.383	0.399	0.669	0.683	0.698	0.554	0.561	0.582	
DGCPN		0.404	0.413	0.420	0.732	0.742	0.751	0.625	0.635	0.654
T2I	CVH (Kumar and Udupa 2011)	0.275	0.236	0.186	0.580	0.579	0.580	0.378	0.378	0.379
	FSH (Liu et al. 2017)	0.367	0.448	0.490	0.589	0.595	0.595	0.395	0.408	0.417
	CMFH (Ding, Guo, and Zhou 2014)	0.495	0.513	0.533	0.590	0.595	0.598	0.487	0.488	0.493
	LSSH (Zhou, Ding, and Guo 2014)	0.403	0.411	0.422	0.621	0.628	0.626	0.476	0.481	0.477
	UGACH (Zhang, Peng, and Yuan 2018)	0.339	0.398	0.418	0.692	0.698	0.699	0.557	0.562	0.580
	DJSRH (Su, Zhong, and Zhang 2019)	0.512	0.536	0.544	0.683	0.694	0.717	0.546	0.568	0.599
	UKD-SS (Hu et al. 2020)	0.400	0.402	0.424	0.704	0.705	0.714	0.587	0.599	0.599
	DSAH (Yang et al. 2020b)	0.527	0.540	0.544	0.707	0.713	0.728	0.621	0.632	0.646
JDSH (Liu et al. 2020)	0.398	0.448	0.480	0.686	0.699	0.716	0.580	0.596	0.626	
DGCPN		0.539	0.550	0.558	0.729	0.741	0.749	0.631	0.648	0.660

Table 1: Performance comparison of ten UCMH methods on three public datasets.

a text query (T2I). The retrieval performance is evaluated using MAP. Given one query and the first R top ranked retrieved data, the average precision (AP) is defined as:

$$AP = \frac{\sum_{q=1}^R P(q)rel(q)}{\sum_{q=1}^R rel(q)}, \quad (13)$$

where $rel(q)=1$ if the item at rank q is relevant, $rel(q)=0$ otherwise. $P(q)$ denotes the precision of the result ranked at q . The MAP is obtained by averaging the AP of all the queries. We report MAP using all retrieval data.

Implementation Details

The layers of similarity-preserving subnetworks are set as $d_I-4096-d_b$ for images and $d_T-4096-d_b$ for texts. We fix the feature-extracting subnetworks' parameters during training and only update the parameters of similarity-preserving subnetworks. We use a mini-batch SGD optimizer with a 0.9 momentum and 0.0005 weight decay. The mini-batch size is set to 32. The learning rate is set to 0.005. For simplicity, we perform a 3-step grid search for the parameters. First, we decide the parameter of the pairwise distance. We set $\gamma=0$, $\lambda_1=\lambda_2=1$, and tune α from 0.01, 0.99, and 0.1 to 0.9 at an increment of 0.1 per step. Then, we search for the parameters of GC. $\lambda_1=\lambda_2=1$. The value of α is fixed according to the value in the first step. For Wikipedia, we tune both k and β from 300 to 1200 at an increment of 300 and γ from 0.01, 0.99, 0.1 to 0.9 at an increment of 0.1 per step. For MIRFlickr-25K and NUS-WIDE, we tune k from 500 to 2000 at an increment of 500, β from 2000 to 4500 at an increment of 500, and γ from 0.01, 0.99, and 0.1 to 0.9 at an increment of 0.1 per step, respectively. We

last tune both λ_1 and λ_2 using the grid search from 0.01 to 10 at a product of 10 per step. We use validation sets with early stopping to determine the parameters. All parameters are determined using 64-bit binary codes. The final parameters are: for Wikipedia: $\alpha=0.3$, $\gamma=0.3$, $\lambda_1=1$, $\lambda_2=1$, $\beta=900$, and $k=600$; for MIRFlickr-25K $\alpha=0.01$, $\gamma=0.3$, $\lambda_1=1$, $\lambda_2=1$, $\beta=4000$, $k=2000$; and for NUS-WIDE: $\alpha=0.1$, $\gamma=0.3$, $\lambda_1=1$, $\lambda_2=1$, $\beta=4500$, $k=2000$.

Performance Comparison

We compare DGCPN with nine UCMH methods: CVH (Kumar and Udupa 2011), FSH (Liu et al. 2017), CMFH (Ding, Guo, and Zhou 2014), LSSH (Zhou, Ding, and Guo 2014), UGACH (Zhang, Peng, and Yuan 2018), DJSRH (Su, Zhong, and Zhang 2019), UKD-SS (Hu et al. 2020), DSAH (Yang et al. 2020b), and JDSH (Liu et al. 2020). UGACH, DJSRH, UKD-SS, DSAH, and JDSH are deep models. Besides, DJSRH, DASH, and JDSH explored data similarities.

We report the MAP of all comparing methods in Table 1. DJSRH, DASH, and JDSH were trained in end-to-end training, whereas the rest of the methods were trained using two-step training, which first extracts cross-modal features and then uses fixed features to train the remaining networks. The best performance in Table 1 is highlighted in bold. An examination of Table 1 shows that DGCPN obtains the best performance on all datasets regardless of the criteria. In particular, DGCPN outperforms the second-best competitor, DSAH, in MIRFlickr-25K by 4.4%, 4.2%, and 4.0% on 16-bit, 32-bit, and 64-bit for I2T and by 3.1%, 3.9%, and 2.9% on 16-bit, 32-bit, and 64-bit for T2I, respectively. In NUS-WIDE, compared with DSAH, DGCPN obtains improvements of 3.8%, 3.8%, and 3.5% on 16-bit, 32-bit, and

	MIRFlickr-25K		NUS-WIDE	
	I2T	T2I	I2T	T2I
Data Similarity Types				
DGCPN-OIPD	0.725	0.724	0.626	0.632
DGCPN-NoPD	0.748	0.748	0.651	0.656
Similarity Preserving Losses				
DGCPN-GL	0.734	0.727	0.631	0.636
DGCPN-GL+CL	0.746	0.749	0.649	0.660
Hashing optimization strategies				
DGCPN-Nhash	0.746	0.731	0.651	0.655
DGCPN-HashL	0.748	0.742	0.653	0.658
DGCPN-Atanh	0.746	0.739	0.656	0.662
DGCPN	0.751	0.749	0.658	0.663

Table 2: Ablations experiments on MIRFlickr-25K and NUS-WIDE.

64-bit for I2T and of 1.6%, 2.5%, and 2.2% on 16-bit, 32-bit, and 64-bit for T2I, respectively. These improvements demonstrate the ability of DGCPN for UCMH.

Ablation Experiments

In table 2, we conduct three types of ablation experiments to discuss the methodological details of DGCPN. For simplicity, we use MIRFlickr-25K and NUS-WIDE as testbeds.

First, we demonstrate the significance of GC for DGCPN. Two variants are proposed. DGCPN-OIPD is the DGCPN only exploits pairwise distances, and DGCPN-NoPD is the DGCPN does not add pairwise distances. An examination of the results presented in Table 2 shows that DGCPN-NoPD outperforms DGCPN-OIPD. The improvements indicate that GC is the key success of DGCPN. DGCPN performs the best, which reveals that adding pairwise distances contributes to robust data similarities.

Then, we verify the usefulness of comprehensive similarity preserving losses. Two variants are developed. DGCPN-GL is the DGCPN that only uses graph-coherence preserving losses, and DGCPN-GL+CL is DGCPN without preserving intra- and inter-modality consistency preserving losses. It is observed that DGCPN-GL shows the worst performance, and DGCPN obtains the best performance. These results demonstrate that exploiting coexistent similarities and intra- and inter-modality consistency alleviates GC’s errors and benefits to the retrieval performance.

Last, we show the necessity of the proposed half-real and half-binary optimization strategy. Three variants are designed for comparison. DGCPN-Nhash is DGCPN without using the half-real and half-binary optimization strategy. DGCPN-Atanh and DGCPN-HashL are DGCPN-Nhash that exploits adjusted Tanh (Yang et al. 2020b) and a hashing function: $\|\mathbf{H} - \mathbf{B}\|_F$, respectively. DGCPN-Atanh and DGCPN-HashL only reduce the value gaps between real values and binary codes. As shown in Table 2, DGCPN shows the best performance. It is necessary to reduce the similarity gaps between real-valued space and Hamming space, and the half-real and half-binary optimization strategy is an ef-

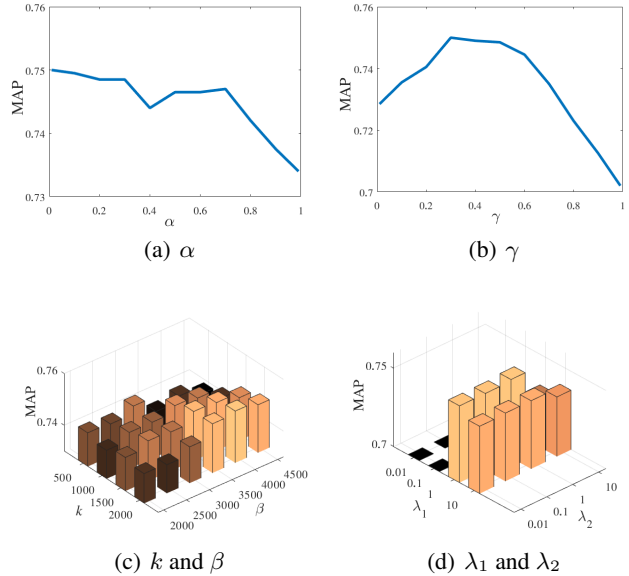


Figure 4: Average MAP of the DGCPN with different parameter values on the MIRFlickr-25K dataset.

fective approach for obtaining an improved retrieval space.

Parameter Sensitivity

Six types of parameters must be adjusted, namely, α , γ , k , β , λ_1 , and λ_2 . In this subsection, we study the performance impacts of these individual parameter values. Fig. 4 shows the average MAP of I2T and T2I with different parameter values on the MIRFlickr-25K datasets with the hash code length of 64 bits. From Fig. 4, we can draw the following conclusions: 1) α indicates the relative significance of image and text features. It is observed that a proper combination of cross-modal distances obtains better performance. 2) γ adjusts the relative significance of the pairwise distances and graph-neighbor coherence. In Fig. 4 (b), we can observe that both higher or lower values of γ result in poor performance. 3) k is the number of the k -nearest neighbor for each node. β is the scale parameter to adjust the range of graph-neighbor coherence. Both parameters contribute to the final value of graph-neighbor coherence. We can see that a proper combination of k and β leads to better performance. 4) λ_1 and λ_2 are the parameters to adjust the relative significance of the three types of similarity preserving losses. It can be concluded that all three types of similarity preserving losses benefit to the final retrieval performance.

Conclusion

In this paper, we develop a novel deep graph-neighbor coherence preserving network (DGCPN) for UCMH. Specifically, DGCPN proposes 1) graph-neighbor coherence to explore relationships between data and their neighbors for more accurate data similarities, 2) comprehensive similarity preserving losses to regulate three types of complementary similarities for robust similarity preserving learning, and 3) a half-

real and half-binary optimization strategy to reduce value gaps and similarity gaps between the real-valued space and Hamming space for better retrieval performance. The experimental results on three publicly available UCMH datasets compared with the state-of-the-art demonstrate the capability of DGCPN for UCMH.

Acknowledgment. This work was supported in part by the National Nature Science Foundation of China: Grant No. 61836002, No. 62002090, and No. 62020106007, in part by the National Key R&D Program of China: Grant No. 2018AAA0100603, and in part by the Australian Research Council Projects: FL-170100117, DP-180103424, and IH-180100002.

References

- Blei, D. M.; Ng, A. Y.; and Jordan, M. I. 2003. Latent dirichlet allocation. *Journal of machine Learning research* 3(Jan): 993–1022.
- Chua, T.-S.; Tang, J.; Hong, R.; Li, H.; Luo, Z.; and Zheng, Y. 2009. NUS-WIDE: a real-world web image database from National University of Singapore. In *Proceedings of the ACM international conference on image and video retrieval*, 1–9.
- Deng, J.; Dong, W.; Socher, R.; Li, L.-J.; Li, K.; and Fei-Fei, L. 2009. Imagenet: A large-scale hierarchical image database. In *2009 IEEE conference on computer vision and pattern recognition*, 248–255. Ieee.
- Ding, G.; Guo, Y.; and Zhou, J. 2014. Collective matrix factorization hashing for multimodal data. In *Proceedings of the IEEE conference on computer vision and pattern recognition*, 2075–2082.
- Fang, Y.; Zhang, H.; and Ren, Y. 2019. Unsupervised cross-modal retrieval via Multi-modal graph regularized Smooth Matrix Factorization Hashing. *Knowledge-Based Systems* 171: 69–80.
- Feng, F.; Wang, X.; and Li, R. 2014. Cross-modal retrieval with correspondence autoencoder. In *Proceedings of the 22nd ACM international conference on Multimedia*, 7–16.
- Hu, D.; Nie, F.; and Li, X. 2018. Deep binary reconstruction for cross-modal hashing. *IEEE Transactions on Multimedia* 21(4): 973–985.
- Hu, H.; Xie, L.; Hong, R.; and Tian, Q. 2020. Creating Something from Nothing: Unsupervised Knowledge Distillation for Cross-Modal Hashing. In *Proceedings of the IEEE/CVF Conference on Computer Vision and Pattern Recognition*, 3123–3132.
- Huiskes, M. J.; and Lew, M. S. 2008. The MIR flickr retrieval evaluation. In *Proceedings of the 1st ACM international conference on Multimedia information retrieval*, 39–43.
- Jiang, Q.-Y.; and Li, W.-J. 2017. Deep cross-modal hashing. In *Proceedings of the IEEE conference on computer vision and pattern recognition*, 3232–3240.
- Krizhevsky, A.; Sutskever, I.; and Hinton, G. E. 2012. Imagenet classification with deep convolutional neural networks. In *Advances in neural information processing systems*, 1097–1105.
- Kumar, S.; and Udupa, R. 2011. Learning hash functions for cross-view similarity search. In *Twenty-second international joint conference on artificial intelligence*.
- Li, C.; Deng, C.; Wang, L.; Xie, D.; and Liu, X. 2019. Coupled cyclegan: Unsupervised hashing network for cross-modal retrieval. In *Proceedings of the AAAI Conference on Artificial Intelligence*, volume 33, 176–183.
- Li, X.; Chen, M.; Nie, F.; and Wang, Q. 2017. A multiview-based parameter free framework for group detection. In *Thirty-First AAAI Conference on Artificial Intelligence*.
- Li, Y.; Chen, X.; Yang, B.; Chen, Z.; Cheng, Z.; and Zha, Z.-J. 2020. DeepFacePencil: Creating Face Images from Free-hand Sketches. In *Proceedings of the 28th ACM International Conference on Multimedia*, 991–999.
- Liang, J.; Li, Z.; Cao, D.; He, R.; and Wang, J. 2016. Self-paced cross-modal subspace matching. In *Proceedings of the 39th International ACM SIGIR conference on Research and Development in Information Retrieval*, 569–578.
- Liong, V. E.; Lu, J.; and Tan, Y.-P. 2018. Cross-modal discrete hashing. *Pattern Recognition* 79: 114–129.
- Liu, H.; Ji, R.; Wu, Y.; Huang, F.; and Zhang, B. 2017. Cross-modality binary code learning via fusion similarity hashing. In *Proceedings of the IEEE Conference on Computer Vision and Pattern Recognition*, 7380–7388.
- Liu, S.; Qian, S.; Guan, Y.; Zhan, J.; and Ying, L. 2020. Joint-modal Distribution-based Similarity Hashing for Large-scale Unsupervised Deep Cross-modal Retrieval. In *Proceedings of the 43rd International ACM SIGIR Conference on Research and Development in Information Retrieval*, 1379–1388.
- Qiao, T.; Zhang, J.; Xu, D.; and Tao, D. 2019a. Learn, imagine and create: Text-to-image generation from prior knowledge. *Advances in Neural Information Processing Systems* 32: 887–897.
- Qiao, T.; Zhang, J.; Xu, D.; and Tao, D. 2019b. Mirrorgan: Learning text-to-image generation by redescription. In *Proceedings of the IEEE Conference on Computer Vision and Pattern Recognition*, 1505–1514.
- Rasiwasia, N.; Costa Pereira, J.; Coviello, E.; Doyle, G.; Lanckriet, G. R.; Levy, R.; and Vasconcelos, N. 2010. A new approach to cross-modal multimedia retrieval. In *Proceedings of the 18th ACM international conference on Multimedia*, 251–260.
- Simonyan, K.; and Zisserman, A. 2014. Very deep convolutional networks for large-scale image recognition. *arXiv preprint arXiv:1409.1556*.
- Song, J.; Yang, Y.; Yang, Y.; Huang, Z.; and Shen, H. T. 2013. Inter-media hashing for large-scale retrieval from heterogeneous data sources. In *Proceedings of the 2013 ACM SIGMOD International Conference on Management of Data*, 785–796.

- Su, S.; Zhong, Z.; and Zhang, C. 2019. Deep joint-semantics reconstructing hashing for large-scale unsupervised cross-modal retrieval. In *Proceedings of the IEEE International Conference on Computer Vision*, 3027–3035.
- Wang, B.; Yang, Y.; Xu, X.; Hanjalic, A.; and Shen, H. T. 2017. Adversarial cross-modal retrieval. In *Proceedings of the 25th ACM international conference on Multimedia*, 154–162.
- Wang, K.; Yin, Q.; Wang, W.; Wu, S.; and Wang, L. 2016. A comprehensive survey on cross-modal retrieval. *arXiv preprint arXiv:1607.06215*.
- Wang, T.; Zhu, L.; Cheng, Z.; Li, J.; and Gao, Z. 2020. Unsupervised deep cross-modal hashing with virtual label regression. *Neurocomputing* 386: 84–96.
- Wu, G.; Lin, Z.; Han, J.; Liu, L.; Ding, G.; Zhang, B.; and Shen, J. 2018. Unsupervised Deep Hashing via Binary Latent Factor Models for Large-scale Cross-modal Retrieval. In *IJCAI*, 2854–2860.
- Xie, D.; Deng, C.; Li, C.; Liu, X.; and Tao, D. 2020. Multi-Task Consistency-Preserving Adversarial Hashing for Cross-Modal Retrieval. *IEEE Transactions on Image Processing* 29: 3626–3637.
- Xie, L.; Zhu, L.; and Chen, G. 2016. Unsupervised multi-graph cross-modal hashing for large-scale multimedia retrieval. *Multimedia Tools and Applications* 75(15): 9185–9204.
- Yang, B.; Chen, X.; Hong, R.; Chen, Z.; Li, Y.; and Zha, Z.-J. 2020a. Joint Sketch-Attribute Learning for Fine-Grained Face Synthesis. In *International Conference on Multimedia Modeling*, 790–801. Springer.
- Yang, D.; Wu, D.; Zhang, W.; Zhang, H.; Li, B.; and Wang, W. 2020b. Deep Semantic-Alignment Hashing for Unsupervised Cross-Modal Retrieval. In *Proceedings of the 2020 International Conference on Multimedia Retrieval*, 44–52.
- Yang, X.; Song, X.; Han, X.; Wen, H.; Nie, J.; and Nie, L. 2020c. Generative Attribute Manipulation Scheme for Flexible Fashion Search. In *Proceedings of the 43rd International ACM SIGIR Conference on Research and Development in Information Retrieval*, 941–950.
- Yu, J.; Rui, Y.; and Chen, B. 2013. Exploiting click constraints and multi-view features for image re-ranking. *IEEE Transactions on Multimedia* 16(1): 159–168.
- Zhai, X.; Peng, Y.; and Xiao, J. 2013. Learning cross-media joint representation with sparse and semisupervised regularization. *IEEE Transactions on Circuits and Systems for Video Technology* 24(6): 965–978.
- Zhan, Y.; Yu, J.; Yu, Z.; Zhang, R.; Tao, D.; and Tian, Q. 2018. Comprehensive distance-preserving autoencoders for cross-modal retrieval. In *Proceedings of the 26th ACM international conference on Multimedia*, 1137–1145.
- Zhang, J.; and Peng, Y. 2019. Multi-pathway generative adversarial hashing for unsupervised cross-modal retrieval. *IEEE Transactions on Multimedia* 22(1): 174–187.
- Zhang, J.; Peng, Y.; and Yuan, M. 2018. Unsupervised Generative Adversarial Cross-Modal Hashing. In *Proceedings of the AAAI Conference on Artificial Intelligence*, volume 32.
- Zhang, J.; and Tao, D. 2020. Empowering Things with Intelligence: A Survey of the Progress, Challenges, and Opportunities in Artificial Intelligence of Things. *IEEE Internet of Things Journal*.
- Zhou, J.; Ding, G.; and Guo, Y. 2014. Latent semantic sparse hashing for cross-modal similarity search. In *Proceedings of the 37th international ACM SIGIR conference on Research & development in information retrieval*, 415–424.